

The influence of translational excitation on the dynamics of the reaction between OH and HCN

Klaus Mikulecky and Karl-Heinz Gericke

*Institut für Physikalische und Theoretische Chemie der Johann Wolfgang Goethe-Universität,
Marie Curie-Strasse 11, D-60439 Frankfurt am Main, Germany*

(Received 4 May 1994; accepted 19 August 1994)

The dynamics of the reaction $\text{OH}(^2\Pi) + \text{HCN} \rightarrow \text{CN}(^2\Sigma) + \text{H}_2\text{O}$ has been investigated at different collision energies between 55.7 and 109.5 kJ/mol with the laser pump-and-probe technique. CN is formed in its electronic and vibrational ground state. Product rotational state distributions and line profiles have been obtained. We determined the partition of the available energy to the degrees of freedom of the products. At low collision energies most of the energy is released as translation, while at high collision energies the internal excitation of the newly formed H_2O molecule dominates the energy balance. The fraction of CN rotational energy remains nearly constant. The effective transfer of reactant translation to product internal excitation indicates that the reaction surmounts an early barrier. Further, absolute reaction cross sections have been determined at two collision energies. © 1994 American Institute of Physics.

I. INTRODUCTION

The reaction dynamics of species carrying a known amount of energy in defined degrees of freedom is an important tool to unravel reaction mechanisms. In general, translational and vibrational degrees of freedom can contain enough energy to induce large effects on the macroscopic kinetics and the reaction product state distribution, as was shown in the fundamental work of Polanyi.^{1,2}

In this article we want to present the results from an investigation of the collision energy dependence of the reaction between hydroxyl radicals, OH, and hydrogen cyanide, HCN:



Reaction (1) is endothermic by 9.5 kJ/mol, so collision energy has to be transferred into the system to let the reaction proceed. The buildup of the product CN has not been observed yet. There was just a rate measurement of the reverse reaction, although Eq. (1) is one step in the combustion of fuel-bound nitrogen to nitrous oxides.³⁻⁷

Although there has been a large number of determinations of the influence of translational energy on the dynamics of elementary reactions, either in molecular beam or in laser experiments, those investigations were restricted to atom-molecule reactions. Reaction (1) is the first reactive process between two molecules where the influence of the collision energy on the dynamics and the absolute reaction cross section is investigated.

A molecular reactant requires special emphasis on the problem of selective energy deposition in the process in which it is produced, because a molecule can carry translational, rotational, and vibrational energy. If the reactant does not carry one type of energy selectively the reaction conditions more and more resemble a simple heating, and no selectivity concerning the energy consumption in the reaction will be observed. A reactant molecule that matches the requirement of selective energy content is OH produced by laser photolysis of H_2O_2 . It has been shown in a number of

experiments that H_2O_2 decays on UV excitation to OH with a very narrow velocity distribution, low rotational, and no vibrational excitation. Experiments concerning the dissociation wavelengths 355,⁸ 266,⁹⁻¹⁶ 248,¹⁷⁻¹⁹ and 193 nm,^{9,10,20-25} and the vacuum ultraviolet²⁶⁻³² are published, data from the 308 and 222 nm dissociation were measured during this work and will be published elsewhere. The narrow velocity distribution and the ease of changing the OH velocity by changing the H_2O_2 dissociation wavelength make the hydroxyl radical an ideal molecular reactant, not only for dynamical experiments but also for the determination of absolute reaction cross sections.

In theory, there have been transition state theory (TST) approximations of the Arrhenius parameters of other channels of the reaction between OH and HCN, namely those leading to $\text{HOCN} + \text{H}$, $\text{HNCO} + \text{H}$, and $\text{NH}_2 + \text{CO}$.³³ No dynamical calculations are currently available for the $\text{CN} + \text{H}_2\text{O}$ channel.

II. EXPERIMENT

The experiments were performed by the pump-and-probe technique, the experimental setup was generally described in a previous paper.³⁴ In a vacuum chamber a mixture of 25% HCN and 75% H_2O_2 at a total pressure of 5 Pa was photolyzed at wavelengths between 308 and 193 nm to yield OH. Excimer (308, 248, 222, and 193 nm) and Nd:YAG (266 nm) lasers were used as photolysis light sources. 100 ns after the initiation of the reaction the probe laser beam was fired into the cell, collinearly to the photolysis beam.

The diameter of the photolysis beam was considerably greater than the diameter of the probe beam so that there are no disturbances due to molecules flying out of the probe region. An excimer-pumped dye laser, operating with the dye QUI, served as the probe beam source. Starting from 388.3 nm the probe beam excited the blue-degraded ($B^2\Sigma^+ \leftarrow X^2\Sigma^+$) band of CN. The laser-induced fluorescence (LIF) was observed by a photomultiplier. After aver-

aging the signal in a boxcar integrator (Stanford Research Systems, Type SR 250) the data were digitized and stored in a computer. A home-built digital delay generator supplied the trigger signals for the lasers and the data acquisition. In order to perform line profile measurements the probe dye laser was equipped with an intracavity étalon. The étalon reduces the linewidth from $\approx 0.3 \text{ cm}^{-1}$ in the grating mode to $\approx 0.06 \text{ cm}^{-1}$ (FWHM) as was determined by linewidth measurements of thermalized CN. Apart from line profile measurements, all spectroscopic experiments were performed in saturation of the CN transition.

III. RESULTS

A. Influences from other processes

Generally, the production of CN is observed only when there are both reactants, H_2O_2 and HCN, present in the reaction cell, but there is one exception: At an initiation wavelength of 193 nm the generation of CN is observed when there is *only* HCN present in the reaction cell. However, the signal intensity is significantly reduced in that case. These CN products exhibit a rotational temperature of 1500 K corresponding to a rotational energy of $E_{\text{rot}}=1040 \text{ cm}^{-1}$. Furthermore, a considerable vibrational excitation was observed. The Doppler linewidth of its transitions was determined to be near the limit of the resolution of our dye laser of 0.06 cm^{-1} which is much narrower than the observed linewidth of CN generated in the reaction of OH with HCN. These features suggest that the CN is generated by the photolysis of HCN, for the CN velocity is very small as it had to be expected in a HCN dissociation.

The photodissociation of HCN at 193 nm yields an available energy of 6200 cm^{-1} to be distributed among the products. Taking into account the energy found as internal excitation of CN, the remaining translational energy corresponds to a velocity of $v_t=450 \text{ ms}^{-1}$, where the thermal velocity of the parent molecule $v_{\text{HCN}}=485 \text{ ms}^{-1}$ still has to be considered. The expected Doppler linewidth of the CN transition is thus $\Delta\nu_D \approx (\nu_0/c) \cdot \sqrt{v_{\text{HCN}}^2 + v_t^2} \approx 0.056 \text{ cm}^{-1}$, what is in fairly good agreement with the experimental observation. So we draw the conclusion that the CN is generated by photodissociation of HCN. The photodissociation dynamics of HCN at 193 nm have recently been investigated by Eng *et al.*³⁵ The authors reported a population ratio of $P(v=0)/P(v=1)=1.7$ and a rotational energy of CN ($v=0$) of 1065 cm^{-1} , which matches our experimental data.

The dissociation at 193 nm does not affect the product state distribution resulting from the reaction between OH and HCN, because its properties are known and were used to correct the data that were measured in the reaction. The influence of the HCN dissociation is restricted to about 10%–15% of the total signal intensity.

B. Product state distribution

Reaction (1) yields CN with a rotational excitation that depends on the collision energy in the system OH+HCN. Figure 1 shows a typical CN spectrum observed after the reaction was initiated at a wavelength of 248 nm. The line intensities from the spectra recorded at different initiation

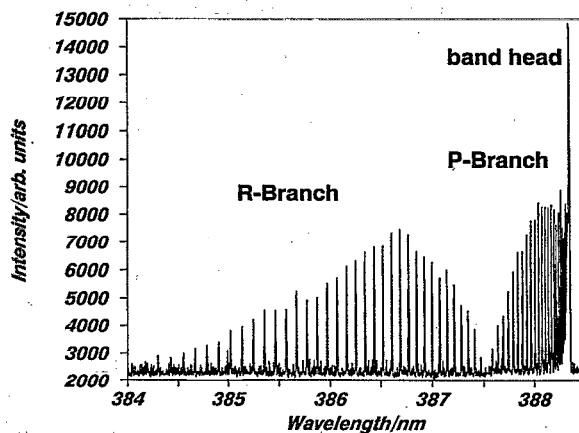


FIG. 1. Typical example of a LIF spectrum of CN generated in Reaction (1).

wavelengths directly yield the population numbers of the rotational states of CN because the transitions were saturated. In Fig. 2 a Boltzmann representation of the CN rotational state distribution is shown. The population of the rotational states decreases monotonically and can be described by a temperature parameter, with a strong influence from the initiation wavelength and therefore from the available energy. The dependence of the rotational energy of CN, E_{rot} on the available energy for the reaction E_{av} is shown in Fig. 3. The rotational excitation of CN increases linearly with E_{av} .

CN has a $^2\Sigma$ ground state, so the spin-rotation splitting of the rotational lines has to be taken into account when performing linewidth measurements and subsequent fit procedures. In lower rotational states the splitting causes a broadening of the lines. At high rotational quantum numbers ($N \geq 40$) the spin components appear resolved. The observation of resolved spin-rotation doublets allows us to state that there is no preponderance of one of the spin components. The magnitude of the splitting is known and was considered

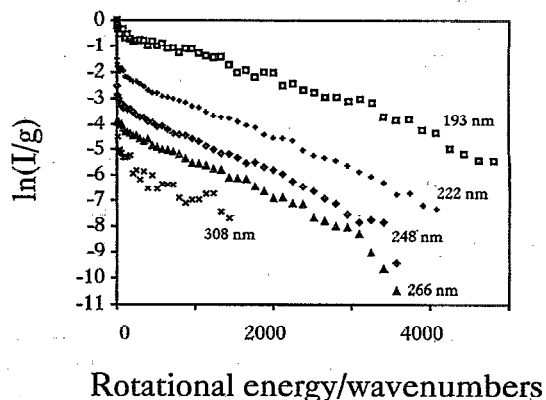


FIG. 2. Boltzmann representation of the rotational distribution of CN($X^2\Sigma$, $v=0$, J) generated by Reaction (1). The points belonging to different wavelengths are displaced by 1.5 units on the logarithmic scale for clarity. g denotes the degeneracy of the rotational states, $g=2J+1$.

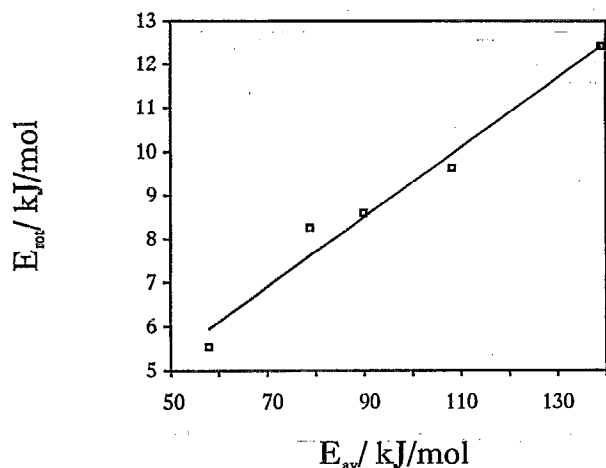


FIG. 3. The dependence of the rotational energy of CN, $E_{rot}(\text{CN})$, on the available energy E_{av} . Energies in kJ/mol.

in the fit, i.e., two profiles were fitted to a single observed line, in order to obtain correct data for the linewidth.³⁶

In order to determine the center-of-mass translational energy of the reaction products CN and H_2O , line profile measurements were performed. This is a much more difficult task than just determining the internal state distribution, for line profile measurements have to be performed at a strictly linear dependence of signal intensity on the probe laser power to avoid power broadening. As a consequence, the fluorescence intensity decreases strongly. To obtain an acceptable S/N ratio extended averaging is necessary in these cases.

For each photolysis wavelength 10 to 15 line profiles were recorded. Doppler and Gauss functions were fit to the profiles. The fit procedure yields the FWHM of the linewidth among other parameters. For further calculations, an average value of the linewidth at $N=10$ was used, which is a strong transition near the population maximum. Table I shows the mean linewidth $\Delta\tilde{\nu}$ of the CN product and the energy data of the reaction. The observed CN Doppler width of $\Delta\tilde{\nu}=0.182\text{ cm}^{-1}$ corresponds to a velocity of $v=c\cdot\Delta\tilde{\nu}/\tilde{\nu}\approx 2100\text{ m/s}$.

C. Reaction cross section

The absolute reaction cross section of Reaction (1) can be determined, when the CN signal intensities from Reaction (1) are compared with signals of a CN source with known absorption cross section and quantum yield. We decided to

use cyanogen, C_2N_2 , as a reference CN precursor, because its photodissociation dynamics at 193 nm is known,^{37,38} as well as the absorption cross section and the quantum yield.³⁹ Further, it is a very clean CN source. The comparison of CN line intensities I from the reaction and from the dissociation is straightforward. The following relations hold (the reaction is indexed r , the dissociation d):

$$I_r \sim P_r(J) \cdot \sigma(\text{H}_2\text{O}_2) \cdot \phi(\text{OH}) \cdot [\text{H}_2\text{O}_2] \cdot [1 - \exp(-k_2[\text{HCN}]\Delta t)], \quad (2)$$

$$I_d \sim P_d(J) \cdot \sigma(\text{C}_2\text{N}_2) \cdot \phi(\text{CN}) \cdot [\text{C}_2\text{N}_2]. \quad (3)$$

The intensity I of CN from the dissociation depends on the concentration of the precursor, the absorption cross section σ , the quantum yield ϕ , and on the relative contribution $P(J)$ of the observed state J with respect to all the states that are populated in the process. Additionally, in the case of the reaction there is the time-dependent expression in brackets to be taken into account. The concentration of the second reactant $[\text{HCN}]$, the time delay Δt between initiation and probe and the second-order rate constant k_2 , have to be considered, the latter being the interesting quantity.

The proportionality constants of Eqs. (2) and (3) are the same, because the experimental conditions are the same for the reaction and the dissociation. There is no flyout of the CN out of the probe region, for the diameter of the photolysis beam was greater than the diameter of the probe beam. The product state distribution $P_d(J)$ of CN generated in the photodissociation of C_2N_2 has also been measured in an additional experimental run. Thus Eqs. (2) and (3) can be readily resolved to yield a value for the rate constant $k_2=5.4\times 10^{-13}\text{ cm}^3\text{ molecule}^{-1}\text{ s}^{-1}$. The rate constant is related to the reaction cross section σ , $k_2=\sigma\cdot v$, where v is the relative reactant velocity of 4560 ms^{-1} . Thus, one obtains a reaction cross section of

$$\sigma = (1.18 \pm 0.02) \times 10^{-18}\text{ cm}^2$$

for a center velocity of 4560 ms^{-1} . The velocity range is essentially influenced by the thermal velocity distribution of the reagent HCN and the OH precursor H_2O_2 . From $\Delta v/v=0.5\cdot\Delta E_{\text{coll}}/E_{\text{coll}}$ we obtain a full width at half-maximum (FWHM) of $\Delta v=940\text{ ms}^{-1}$.

Similar measurements have been performed at the initiation wavelength of 222 nm. The absorption cross section of C_2N_2 at 222 nm is not published yet, so we determined $\sigma(222\text{ nm})$ in a separate experiment. We measured the absorption of the KrCl laser beam passing the vacuum chamber

TABLE I. E_{exc} represents the OH excess energy in the photodissociation of H_2O_2 , the collision energy of the reactants is given by E_{coll} , E_{av} is the available energy of the reaction, and E_{rot} is the rotational energy of CN and OH, respectively. ΔE_{coll} denotes the distribution width FWHM of the collision energy (Ref. 42). Additionally the measured Doppler linewidths of the CN transitions are given here ($\Delta\tilde{\nu}$). At the photolysis wavelength of 308 nm no line profile measurement could be performed. All energies in kJ/mol.

λ (nm)	E_{exc}	E_{coll}	ΔE_{coll}	$E_{rot}(\text{OH})$	E_{av}	$E_{rot}(\text{CN})$	$\Delta\tilde{\nu}$ (cm^{-1})
308	172.8	55.7	31.7	6.7	55.4	3.5	...
266	222.3	70.7	35.9	12.5	76.2	8.3	0.175
248	249.2	79.3	38.1	15.0	87.2	8.6	0.176
222	295.9	93.7	41.5	18.9	105.6	9.6	0.182
193	350.3	109.5	45.1	33.5	136	12.4	0.179

TABLE II. Partitioning of energy into the different degrees of freedom.

Energies (kJ/mol)	H_2O_2 photolysis wavelength (nm)				
	308	266	248	222	193
$E_{\text{rot}}(\text{OH})$	6.7	12.5	15	18.9	33.5
$E_{\text{trans}}(\text{OH})$	86.4	111	125	148.4	175
E_{av}	55.4	76.2	87.2	105.6	136
E_{coll}	55.7	70.7	79.2	93.7	109.5
$E_{\text{rot}}(\text{CN})$	5.5	8.3	8.6	9.6	12.4
$E_{\text{trans}}(\text{CN})$...	26.4	23.7	22.1	14.4
$E_{\text{int}}(\text{H}_2\text{O})$...	3.5	20.8	42.0	88.4
$E_{\text{trans}}(\text{H}_2\text{O})$...	38.1	34.2	31.9	20.8
$f_{\text{rot}}(\text{CN})$	0.10	0.11	0.10	0.09	0.09
$f_{\text{int}}(\text{H}_2\text{O})$...	0.05	0.24	0.40	0.65
f_{trans}	...	0.84	0.66	0.51	0.26

filled with C_2N_2 at different pressures. The absolute cross section $\sigma(\text{C}_2\text{N}_2, 222 \text{ nm})$ is then obtained readily from the Lambert-Beer equation. We found a value of $\sigma = 6.3 \times 10^{-23} \text{ cm}^2$.

Determination of the CN product state distribution from the C_2N_2 dissociation is straightforward. Unfortunately, no quantum yield $\phi(\text{CN})$ is known for the C_2N_2 dissociation at 222 nm, as is required by Eq. (3). So, only a relative value for the cross section could be obtained:

$$\sigma = (6.2 \pm 1.4) \times 10^{-18} \cdot \frac{\phi(\text{CN})}{\phi(\text{OH})} \text{ cm}^2. \quad (4)$$

The quantum yield ratio $\phi(\text{CN})/\phi(\text{OH})$ is estimated to be smaller than 1: $\phi(\text{OH})$ equals nearly 2, and $\phi(\text{CN})$ is expected to be rather small because of the very strong fluorescence that is observed when C_2N_2 is irradiated at a wavelength of 222 nm. We conclude a decrease in σ when changing the collision energy from 110 to 93.7 kJ/mol. In order to obtain additional data on the C_2N_2 dissociation we intend to compare the CN production from C_2N_2 at 222 nm to that of BrCN at the same wavelength.

IV. DISCUSSION

A. Partitioning of energy

From the rotational state distribution and the linewidth of the CN product the partitioning of energy among the degrees of freedom of the collision system can be calculated. Conservation of energy requires the validity of the following equation:

$$\begin{aligned} E_{\text{av}} &= \Delta H^\circ + E_{\text{coll}} + E_{\text{int}}(\text{HCN}) + E_{\text{rot}}(\text{OH}) \\ &= E_{\text{rot}}(\text{CN}) + E_{\text{int}}(\text{H}_2\text{O}) + E_{\text{trans c.m.}}(\text{CN}, \text{H}_2\text{O}). \end{aligned} \quad (5)$$

E_{av} consists of the contributions given by the internal or rotational energies of the reactants, $E_{\text{int}}(\text{HCN})$ and $E_{\text{rot}}(\text{OH})$, the endothermicity ΔH° , and the translational energy of the reactants E_{coll} in the center-of-mass system. An exact calculation of the average collision energy requires a careful treatment of initial thermal motion of precursor molecules.⁴⁰⁻⁴² Van der Zande *et al.*⁴² have shown that the average collision energy in hot atom reactions (where the atom is generated in a photodissociation process, similar to OH production in the

present experiment) is readily estimated and is only slightly affected by thermal motions of the precursor (H_2O_2) and target (HCN) molecule. However, the width of the energy distribution depends significantly on the width of the thermal velocity distribution. The average collision energy between OH and HCN is calculated by the equation

$$E_{\text{coll}} = \frac{1}{2} \mu \cdot [v_{\text{OH}}^2 + v_{\text{HCN}}^2 + v_{\text{H}_2\text{O}_2}^2] \quad (6)$$

and is listed in Table I for the different photolysis wavelengths. μ represents the reduced mass of the OH+HCN system.

The width (FWHM) of the collision energy ΔE_{coll} is derived from the work of van der Zande *et al.*⁴² and is given by the equation

$$\Delta E_{\text{coll}} = \left[\frac{4m_{\text{HCN}}(2m_{\text{OH}} + m_{\text{HCN}})}{(m_{\text{OH}} + m_{\text{HCN}})^2} \cdot kT \cdot E_{\text{exc}} \cdot \ln 2 \right]^{1/2}, \quad (7)$$

where E_{exc} is the total excess energy in the H_2O_2 photolysis which is released as OH translation. ΔE_{coll} is listed in the third column of Table I.

It is an important result of the calculation that the collision energy of OH and HCN is not defined as sharp as one would expect for the high translational energy of OH. Although the spread in collision energy is still smaller than the average collision energy any sharp energy dependent variation of the cross section will be smoothed out.

Now the right-hand side of Eq. (5) will be evaluated. $E_{\text{int}}(\text{CN})$ can be measured directly as $E_{\text{rot}}(\text{CN})$ since no vibrationally excited CN is observed. There are greater difficulties in determining the center-of-mass (c.m.) translational energy of the reaction products H_2O and CN. The mean velocity of the CN product in the laboratory frame is known from the Doppler linewidth measurements (Table I), and this lab velocity has to be converted into the c.m. system. The latter has the great advantage that the velocities of CN and H_2O depend only on their masses, for their linear momenta have to be equal except for the sign. The conversion is described in the Appendix. It should be mentioned that an uncorrelated product recoil direction with respect to the direction of the reactants is assumed. The results of the lab-c.m. conversion are the c.m. translational energies of CN and

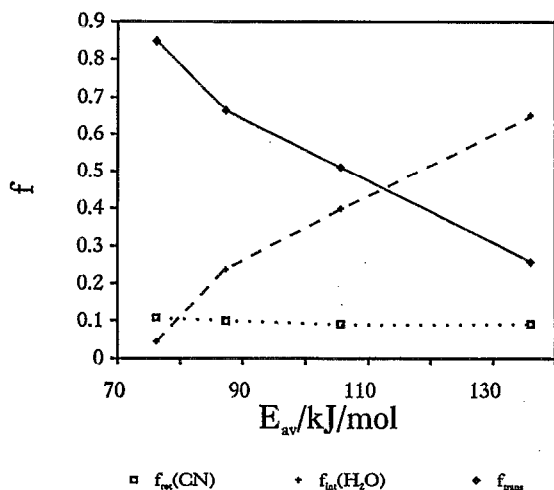


FIG. 4. The partition of energy among the CN rotation f_{rot} , the product translation f_{trans} , and the internal excitation of H_2O , f_{int} .

H_2O . These are the missing values for the determination of the total energy partitioning. The results are shown in Table II.

In Fig. 4 the fraction of the available energy which is distributed among the different degrees of freedom (f data of Table II) is plotted against the available energy. The rotational energy of the CN product holds about 10% of E_{av} , this fraction remains constant as the available energy is varied. A very interesting feature of the energy partition is the fraction of E_{av} released as internal energy of the H_2O product molecule. This fraction rises from 5% at the lowest collision energy to 65% at the highest energy. The effective transfer of collision energy into internal energy of H_2O has to be related to the fact that the H_2O molecule contains the newly formed chemical bond.

B. The reaction mechanism

In general, there are several possible reaction mechanisms to be considered. These are the stripping mechanism, a direct reaction, and the formation of a long living collision complex. In a stripping event the light H atom would be exchanged between the reaction partners without formation of a collision complex. There just has to be an attractive interaction that causes the H-CN bond to be broken so that HO-H can be formed. In that case one would assume that the CN bond will be essentially unaffected and independent of the collision energy. In the experiment we observed that the fraction of E_{av} released as internal motion of CN remains constant at a rather low level and CN acts as a spectator in the reactive collision. The CN bond seems to remain unaffected as the reaction proceeds. In this context a pure stripping process seems to be the adequate description of the reaction mechanism. However, it has to be admitted that this type of reaction is not very likely in our case. The reaction of OH with HCN is endothermic, so it may only proceed when there is some additional energy given to the OH+HCN system, as can be achieved by a real collision. Furthermore, the

observed reaction cross section is roughly three orders of magnitude lower than the gas kinetic cross section. This value is extremely unlikely for a stripping mechanism. Another argument against a predominant role of stripping is the velocity we have to expect for the CN radical in this case. Because of conservation of energy and linear momentum the equations

$$m_{OH}v_{OH} = m_{H_2O}v_{H_2O} + m_{CN}v_{CN}, \quad (8)$$

$$m_{OH}v_{OH}^2 = m_{H_2O}v_{H_2O}^2 + m_{CN}v_{CN}^2, \quad (9)$$

hold in the limiting case of a stripping process where the velocities are related to the lab frame. For simplification, we neglected the contribution of HCN. This causes no substantial error because HCN has a rather low thermal velocity. Equations (8) and (9) may be combined to yield an expression for the product velocities of H_2O and CN (m_{tot} is the sum of masses of the products):

$$v_{H_2O} = v_{OH} \cdot \frac{m_{OH}}{m_{tot}} \cdot \left(1 + \left(1 + \frac{(m_{CN} - m_{OH}) \cdot m_{tot}}{m_{OH} \cdot m_{H_2O}} \right)^{1/2} \right), \quad (10)$$

$$v_{CN} = v_{OH} \cdot m_{OH} / m_{CN} - v_{H_2O} \cdot m_{H_2O} / m_{CN}. \quad (11)$$

So the linear momenta of H_2O and CN just depend on the momentum of OH, the complicated expression containing all the masses is a constant. As an example we may calculate the velocities of H_2O and CN produced by an incident OH molecule with a velocity of 4180 m/s, as it comes out of a H_2O_2 dissociation at 222 nm. Then the H_2O velocity should be 4000 m/s, and that of CN just 75 m/s. If we take the thermal velocity of HCN into account we would expect a CN velocity of about 500 m/s. This is much slower than all measured velocities.

For a direct reaction and a collision complex the linear momenta of H_2O and CN are identical in the c.m. frame:

$$P_{H_2O} = -P_{CN}. \quad (12)$$

The magnitude of the momentum is determined by the amount of energy ΔE that can be transferred to the translational degree of freedom:

$$p_{H_2O} = p_{CN} = \sqrt{2\Delta E \cdot \mu(H_2O, CN)}. \quad (13)$$

If ΔE is the energy that is not transferred into CN rotation [$=E_{av} - E_{rot}(CN)$], then Eq. (13) yields the maximum linear momentum and velocity of the reaction products in the c.m. system. These have to be converted to the laboratory system. For the example of a reaction initiated by the H_2O_2 photolysis at 222 nm the c.m. velocities (2510 and 1740 m/s) yield maximum laboratory frame velocities for H_2O and CN of 4450 and 3680 m/s, respectively. 3680 m/s is much faster than the experimentally determined value of 2100 m/s, but the simple calculation does not account for the energy transferred to the internal degrees of freedom of H_2O . The agreement between the calculation and the experimental values is by no means perfect, but it is far better than between the stripping result and the experiment.

A long living collision complex implies that the energy will statistically be distributed among all degrees of freedom.

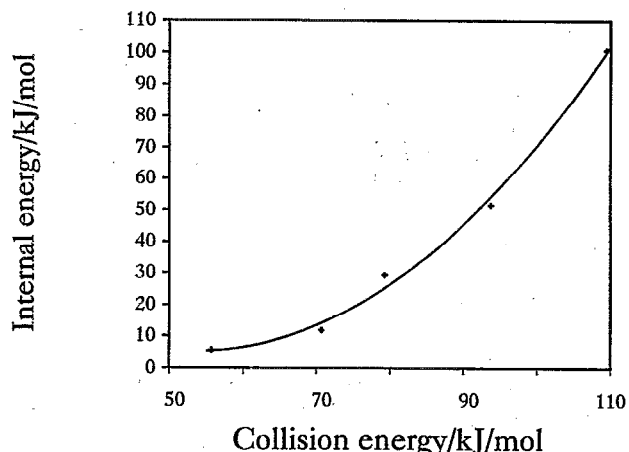


FIG. 5. The total internal excitation of the reaction products CN and H₂O, $E_{\text{int,tot}}$, as a function of the collision energy E_{coll} . The line is a second-order polynomial fit to the experimental data.

Only final state interaction on the exit channel of the reaction may influence this energy distribution. In any case a significant internal excitation of the CN product is expected. Although the internal excitation increases with collision energy (Fig. 3), the CN vibration is not excited at all. Even at the highest collision energy (193 nm photolysis of H₂O₂) no vibrationally excited CN is generated in the bimolecular reaction. Consequently it seems to be very likely that the reaction proceeds directly where not sufficient time is left for an energy transfer into CN vibration. For a direct reaction one can distinguish between the "old" CN bond in the reagent HCN and the "new" H–OH bond. The new bond should contain most of the released energy and the internal energy of H₂O should increase with increasing collision energy. In fact, this behavior is observed in the experiment (Table II, Fig. 4).

From the data it is possible to estimate the barrier height. Figure 5 shows a plot of the total internal energy of the products [i.e., $E_{\text{rot}}(\text{CN}) + E_{\text{int}}(\text{H}_2\text{O})$] against the collision energy E_{coll} . The solid line is a second-order polynomial fit to the experimental data. The fit reaches a minimum at ~ 53 kJ/mol. We conclude that this is the energy that has to be surmounted to initiate the reaction. It should be emphasized that this is only an estimate of the barrier height. However, the temperature dependence of the reverse reaction has been determined⁵ and from that observation an activation barrier of 45 kJ/mol has been calculated for Reaction (1). The fairly good agreement between our experimental data and that of Szekely *et al.*⁵ shows that the correlation between the collision energy and the internal energy of the products is related to the activation barrier of the reaction.

The question whether this barrier is rather early or late is speculative, but may be discussed by evaluating the partitioning of energy among the different degrees of freedom of the products. It has been shown that at large collision energies the available energy is transferred essentially into internal energy of H₂O. This behavior is more typical for reac-

tions with an early barrier, where translational motion of the reagent is transferred into vibrational motion of the product.

ACKNOWLEDGMENTS

The authors wish to thank Professor Dr. J. B. Halpern for the supply of the C₂N₂ absorption data, and Professor Dr. F. J. Comes for helpful discussions and material support. This work was performed as part of a program of the Deutsche Forschungsgemeinschaft.

APPENDIX

The velocity v of the products in the laboratory frame is connected to their velocity w in the c.m. system via

$$\mathbf{v} = \mathbf{v}_{\text{c.m.}} + \mathbf{w}, \quad (\text{A1})$$

where the c.m. velocity $v_{\text{c.m.}}$ is given by

$$v_{\text{c.m.}} = v_{\text{OH}} \cdot \mu / m_{\text{HCN}} + v_{\text{HCN}} \cdot \mu / m_{\text{OH}}. \quad (\text{A2})$$

From Eq. (A1) follows

$$v^2 = v_{\text{c.m.}}^2 + w^2 - 2v_{\text{c.m.}}w \cdot \cos \Theta, \quad (\text{A3})$$

where Θ is the angle between $\mathbf{v}_{\text{c.m.}}$ and \mathbf{w} .

If the product recoil direction is not correlated with the direction of $\mathbf{v}_{\text{c.m.}}$, then the cosine expression in Eq. (A3) vanishes for mean velocities.

It should be mentioned that for an exact calculation of average energies the collision energy distribution has to be taken into account which is influenced by thermal motion of the reagents. However, van der Zande *et al.*⁴² have shown that the average energies can be readily estimated and are only slightly effected by thermal motion.

The translational energy $E_{\text{c.m.}}(\text{CN})$ of CN in the c.m. system is given by

$$E_{\text{c.m.}}(\text{CN}) = 1/2 \cdot m_{\text{CN}} w_{\text{CN}}^2. \quad (\text{A4})$$

For uncorrelated ($\mathbf{v}_{\text{c.m.}}$, \mathbf{w}) directions one obtains

$$E_{\text{c.m.}}(\text{CN}) = 1/2 \cdot m_{\text{CN}} \cdot [v_{\text{CN}}^2 - (v_{\text{OH}} \mu / m_{\text{HCN}})^2 - (v_{\text{HCN}} \mu / m_{\text{OH}})^2] \quad (\text{A5})$$

and due to conservation of linear momentum ($p_{\text{H}_2\text{O}} = p_{\text{CN}}$):

$$E_{\text{c.m.}}(\text{H}_2\text{O}) = E_{\text{c.m.}}(\text{CN}) \cdot m_{\text{CN}} / m_{\text{H}_2\text{O}}. \quad (\text{A6})$$

The average velocity of CN in the laboratory frame v_{CN} can be obtained from an analysis of the line profile.

¹J. C. Polanyi, *Acc. Chem. Res.* **5**, 161 (1972).

²J. C. Polanyi, *Science* **236**, 680 (1987).

³L. F. Phillips, *Aust. J. Chem.* **32**, 2571 (1979).

⁴A. Jacobs, M. Wahl, R. Weller, and J. Wolfrum, *Chem. Phys. Lett.* **144**, 203 (1988).

⁵A. Szekely, R. K. Hanson, and C. T. Bowman, *Int. J. Chem. Kinet.* **16**, 1609 (1984).

⁶B. S. Haynes, *Combust. Flame* **28**, 113 (1977).

⁷J. Warnatz, *Brennstoff Wärme Kraft* **37**, 11 (1985).

⁸T. M. Ticich, M. D. Likar, H. R. Dübal, L. J. Butler, and F. F. Crim, *J. Chem. Phys.* **87**, 5820 (1987).

- ⁹F. J. Comes, K.-H. Gericke, A. U. Grunewald, and S. Klee, *Ber. Bunsenges. Phys. Chem.* **92**, 273 (1988).
- ¹⁰K.-H. Gericke, A. U. Grunewald, S. Klee, and F. J. Comes, *J. Chem. Phys.* **88**, 6255 (1988).
- ¹¹S. Klee, K.-H. Gericke, and F. J. Comes, *J. Chem. Phys.* **85**, 40 (1986).
- ¹²K.-H. Gericke, S. Klee, F. J. Comes, and R. N. Dixon, *J. Chem. Phys.* **85**, 4463 (1986).
- ¹³R. N. Dixon, J. Nightingale, C. M. Western, and Y. Yang, *Chem. Phys. Lett.* **151**, 328 (1988).
- ¹⁴K.-H. Gericke, S. Klee, and F. J. Comes, *Chem. Phys. Lett.* **137**, 510 (1987).
- ¹⁵K.-H. Gericke, *Faraday Discuss. Chem. Soc.* **82**, 41 (1986).
- ¹⁶S. Klee, K.-H. Gericke, and F. J. Comes, *Ber. Bunsenges. Phys. Chem.* **92**, 429 (1988).
- ¹⁷M. P. Docker, A. Hodgson, and J. P. Simons, *Chem. Phys. Lett.* **128**, 264 (1986).
- ¹⁸J. August, M. Brouard, M. P. Docker, A. Hodgson, C. J. Milne, and J. P. Simons, *Ber. Bunsenges. Phys. Chem.* **92**, 264 (1988).
- ¹⁹M. P. Docker, A. Hodgson, and J. P. Simons, *Faraday Discuss. Chem. Soc.* **82**, 25 (1986).
- ²⁰A. U. Grunewald, K.-H. Gericke, and F. J. Comes, *J. Chem. Phys.* **89**, 345 (1988).
- ²¹K.-H. Gericke, *Phys. Rev. Lett.* **60**, 561 (1988).
- ²²K.-H. Gericke, H. G. Gläser, C. Maul, and F. J. Comes, *J. Chem. Phys.* **92**, 411 (1990).
- ²³F. J. Comes, *Faraday Discuss. Chem. Soc.* **82**, 43 (1986).
- ²⁴A. U. Grunewald, K.-H. Gericke, and F. J. Comes, *J. Chem. Phys.* **87**, 5709 (1987).
- ²⁵A. U. Grunewald, K.-H. Gericke, and F. J. Comes, *Chem. Phys. Lett.* **132**, 121 (1986).
- ²⁶M. Suto and L. C. Lee, *Chem. Phys. Lett.* **98**, 152 (1983).
- ²⁷L. T. Molina and M. J. Molina, *J. Photochem.* **15**, 97 (1981).
- ²⁸H. Gölsenleuchter, K.-H. Gericke, F. J. Comes, and P. F. Linde, *Chem. Phys.* **89**, 93 (1984).
- ²⁹H. Gölsenleuchter, K.-H. Gericke, and F. J. Comes, *Chem. Phys. Lett.* **116**, 61 (1985).
- ³⁰K.-H. Gericke, H. Gölsenleuchter, and F. J. Comes, *Chem. Phys.* **127**, 399 (1988).
- ³¹S. Klee, K.-H. Gericke, H. Gölsenleuchter, and F. J. Comes, *Chem. Phys.* **139**, 415 (1989).
- ³²U. Gerlach-Meyer, E. Linnebach, and K. Kleinermanns, *Chem. Phys. Lett.* **133**, 113 (1987).
- ³³J. A. Miller and C. F. Melius, *Symp. Int. Combust. Proc.* **21**, 919 (1988).
- ³⁴K. Mikulecky and K.-H. Gericke, *J. Chem. Phys.* **96**, 7490 (1992).
- ³⁵R. Eng, T. Carrington, C. H. Dugan, S. V. Filseth, and C. M. Sadowski, *Chem. Phys.* **113**, 119 (1987).
- ³⁶N. Suchard, *Spectroscopic Data IA, IFI* (Plenum, New York, 1975).
- ³⁷J. B. Halpern and W. M. Jackson, *J. Phys. Chem.* **86**, 973 (1982).
- ³⁸A. Schiffmann, D. D. Nelson, and D. J. Nesbitt, *J. Chem. Phys.* **98**, 6935 (1993).
- ³⁹J. B. Halpern (private communication).
- ⁴⁰P. J. Chantry, *J. Chem. Phys.* **55**, 2746 (1971).
- ⁴¹R. B. Bernstein, *Comments At. Mol. Phys.* **4**, 43 (1973).
- ⁴²W. J. van der Zande, R. Zhang, R. N. Zare, K. G. McKendrick, and J. J. Valentini, *J. Phys. Chem.* **95**, 8205 (1991).